

PARALLEL ACQUISITION OF RADIAL VELOCITIES AND METALLICITIES FOR A GAIA-TYPE INTERFEROMETRIC ASTROMETRY MISSION

F. Favata, M.A.C. Perryman

Astrophysics Division, ESTEC, 2200AG Noordwijk, The Netherlands

ABSTRACT

We discuss some possible options for the parallel acquisition of non-astrometric data in the framework of an astrometric experiment such as the proposed GAIA mission. We concentrate on the acquisition of spectroscopic information, discussing the scientific rationale for the proposed measurements, in particular of precise (≈ 1 km/s) radial velocity and metallicity (≈ 0.1 dex) determination. We analyze the performance of a simple slitless scanning spectrograph system, discussing both space and ground-based options, showing that, even without careful optimization such a system could have a performance not too far away from that required to measure all the stars in the sky down to $V \approx 15$ in the lifetime of the proposed GAIA mission. Such an instrument would greatly enhance the scientific capabilities of an astrometric mission, allowing the determination of 3-d space motions as well of important physical parameters for an unprecedented sample of stars.

Keywords: radial velocities; space astrometry; GAIA; spectral classification; abundances.

1. INTRODUCTION

The problem of parallel acquisition of non-astrometric data in the framework of an interferometric astrometry mission such as the proposed GAIA mission was first raised by Perryman (1994) who drew attention to the importance of the question, and demonstrated that acquisition of ‘auxiliary’ data on the scale demanded by the GAIA mission would be a challenging issue. The possibility of acquiring the necessary spectral data through a dedicated ground-based multi-fibre spectroscopic facility was briefly considered. Here we consider an alternative approach, based on a scanning slit-less spectrograph, which could either be incorporated within the satellite payload, or considered as a separate ground-based instrument.

2. WHICH KIND OF DATA

What kind of auxiliary information would it be desirable to acquire in the framework of a mission such as GAIA? Assuming that medium-band (i.e., Strömgren-like) photometry will be acquired already on the focal plane of the interferometers (see Lindgren & Perryman 1994), we have identified three main scientific parameters which would be desirable to acquire for each of the stars for which GAIA will measure the astrometric parameters. Specifically, these are the radial velocity, the metallicity, and the MK spectral type. The rationale for each of the three measurements is described in the following sections.

2.1. Radial Velocity

An interferometric mission such as GAIA will measure both precise distances and proper motions. The third component of the space motion, i.e., the radial velocity, is however necessary to get a complete description of the space motions of the targets, and therefore to be able to carry out 3-d dynamical studies. The usefulness of radial velocity information in the context of an astrometric mission is demonstrated by the large number of ground-based radial velocity measurement programmes being carried out on Hipparcos targets, including two ESO key projects, see Mayor et al. (1989) and Gerbaldi et al. (1989). While an ad hoc approach has been adopted in the case of Hipparcos (involving $\approx 100\,000$ stars), only a dedicated programme could be considered in the context of the 50 million or so stars which could be observed by GAIA.

To be maximally useful, the radial velocity measurements should match the precision of the astrometric measurements. The $10 \mu\text{as/yr}$ which is the GAIA goal translates, at 10 kpc, to about 0.5 km/s. A radial velocity acquisition programme should therefore aim for an accuracy of 1 km/s or better. Using current digital cross-correlation methods radial velocities can be extracted, at least for late-type stars with a spectrum rich in spectral lines, to a precision corresponding to about 1/10 of pixel (Batten 1985). Working in the red region of the spectrum (where the sensitivity of current digital detectors is greater) this translates into a spectral dispersion of about 10 km/s per pixel, or about $R = 30,000$, i.e., the typical resolution of an echelle spectrograph.

Working on Pop II stars Carney et al. (1987) have shown that the digital cross-correlation technique is capable of extracting radial velocities to 1/10 of a pixel on spectra with S/N per pixel as low as 5, using only one echelle order (about 40 Å spectral coverage). This translates, in the space-based baseline design discussed here, into ≈ 700 m/s accuracy. Additionally, they showed that the same spectra could be used to determine the metallicity to about 0.12 dex. We have therefore considered as our goal an instrument which should be able to produce a spectrum with a S/N of 5 per pixel during the mission for the fainter of the GAIA target stars (which we have assumed to be $V \approx 15$). Note that for high S/N spectra (such as the ones the instrument described here would produce for the brighter stars), radial velocities precise to 1/100 of a pixel can be extracted (Campbell et al. 1988), i.e. a factor of 10 better than possible on the weaker objects (or ≈ 70 m/s accuracy in our space-based baseline design). Note that the motion of the Sun-Jupiter barycenter is about 12 m/s, i.e. lower than what it would be achievable at the type of spectral resolutions discussed here.

For determining the radial velocity of solar type stars (i.e., from early F to the coolest stars) the choice of the precise spectral region is not critical, as long as it includes some reasonably strong metallic lines. The region around the Li I 6707.8 Å line would perhaps be a good choice because on spectra with higher S/N it would allow, in addition, a determination of the lithium abundance. Given the importance of lithium as an age indicator, and the usefulness of lithium depletion as a probe of the evolution of the internal structure of solar type stars (see for example Pinsonneault et al. 1990 for the theoretical aspects and Soderblom et al. 1993 for a discussion of some of the observations aspects), this would be an additional measurement which could be useful to trace the younger stars in the large population surveyed by GAIA.

Additional consideration must be given to the best region to survey for the early-type stars, which have very few if any metallic lines. One possibility would be to use a region centred on a Balmer line (typically $H\alpha$ to maximize throughput for the later spectral types). One problem with this choice is the poor performance in the case of emission-line stars, which are a large fraction at the later spectral types (i.e., dMe stars). Clearly, the choice of the ‘best’ spectral region will require some further thought. One attractive possibility would be to simultaneously sample two (or more) specific spectral regions, perhaps through two independent detectors. One such possibility is described in Sec 8.4.

A second, independent reason to sample the radial velocity a large number of times, both on a short and a long time scale (i.e., from about 1 day to about 1 year) to search for binaries, both short and long period. Given that a mission such as GAIA will observe each object several times, this should in principle be possible for at least the brighter objects, for which a single scan provides enough counts in a spectrum to produce a reliable radial velocity determination. This ‘single scan’ limit will be investigated quantitatively later.

A third significant reason for considering the radial

velocities in the context of the astrometric mission is related to the problem of perspective acceleration: the perspective acceleration due a radial velocity V_r is given by $a = -2.0 \times 10^{-9} \pi \mu V_r$, where a is the acceleration in mas/yr^2 , π is the parallax in mas, μ is the proper motion in mas/yr , and V_r is the radial velocity in km/sec .

For a mission duration of t years, the integrated positional error is $e = \frac{1}{2} a (t/2)^2$ mas, reckoned from the central measurement epoch. For Hipparcos, attempts have been made to eliminate systematic errors (including perspective acceleration, by incorporating known radial velocities of affected stars) at the level of 0.1 mas, in view of a nominal mission accuracy of 1 mas. We can assess the effect of unknown radial velocities in the case of GAIA, where current estimates of the astrometric accuracy lie somewhere in the range 1–10 microarcsec, at least for the brightest stars. If we assume a mission duration of 4 years (as for Hipparcos), the threshold radial velocity at which perspective acceleration becomes a significant effect is therefore a factor of 100–1000 times smaller than for Hipparcos, for any given product of $\mu \times \pi$, decreasing further as the square of the actual mission duration. Note that we cannot rely on the astrometric measurements to provide an estimate of the perspective acceleration, and hence deduce the radial velocity of the star—the importance of double and multiple systems, especially amongst the nearest stars, and the associated implications for mass determinations and related orbital studies, means that for GAIA, the disentangling of true orbital accelerations and perspective accelerations will be a very important consideration.

We have used the Hipparcos preliminary estimates of π and μ to estimate the number of objects possibly affected. At the level of 1 microarcsec, some 500 Hipparcos objects would be affected if their $V_r > 10$ km/sec, and some 7000 if $V_r > 100$ km/sec. If we estimate the completeness of the Hipparcos Catalogue within 100 pc at, say, 20 per cent, the number of GAIA stars affected would be a factor of 5 larger. If we require correction at 0.1 microarcsec, some 35 000 stars would be affected if their $V_r > 10$ km/sec, and some 200 000 if $V_r > 100$ km/sec.

The number of stars actually affected clearly depends on the kinematic properties of the various populations sampled by the mission: however, provision must be made to ensure that the higher velocity stars (in particular, both the spheroidal component objects, and the white dwarfs and the long-period variable stars within the disk-population) are not subject to an astrometric bias due to their unknown radial velocities.

2.2. Metallicity

The determination of the metallicity is obviously important to separate the different population which are going to be observed by GAIA, and to possibly study, for example, the relationship between metallicity and kinematics. For separating disk and halo stars (and to possibly separate thin and thick disk population stars) a precision of 0.2 dex should be sufficient.

Metallicity can be determined either on a high-resolution spectrum or on a low-resolution (classification-like) spectrum. Carney et al. 1987 have shown that the same low S/N spectra that they have used for the determination of radial velocity can also be used, by simple χ^2 fitting to a set of template spectra, to determine the global metallicity of the star to about 0.12 dex. In spectra of higher S/N (i.e., 20 or better) the error in the metallicity determination decreases to 0.08 dex. Therefore the same spectra used for the determination of the radial velocity can be used to determine the metallicity.

2.3. Spectral Classification

The two-dimensional MK spectral type is undoubtedly one of the classic parameters which are used to classify a star, being directly linked (at least in solar abundance stars) with the effective temperature and surface gravity. While it is not obvious if and how much the traditional MK classification can (or should) be extended into the domain of metal poor stars (of which a GAIA-type mission will observe a large number), where the line strength will depend on both luminosity class and metal abundance, it is clear that classification-type spectra supply astrophysically useful information, for example, on the presence of emission lines (for example the Balmer series or the CaII H&K doublet), which are a strong indication of stellar activity, or on the presence of abundance anomalies (like, for example, in Ap and Am stars).

To allow a reliable determination both of spectral peculiarities and abundance anomalies, a low resolution spectrum should have a resolution of at least 2 Å per pixel. Also, a large spectral coverage is desirable to include as many as possible ‘interesting’ spectral features and to allow reliable study of the complete HR diagram. In our baseline design we will therefore assume 3000 Å spectral coverage and 1.5 Å per pixel resolution. The final choice of the spectral resolution should be based on extensive simulation to determine the possibility, for example, of determining CNO abundance (and anomalies) as well as Fe peak element abundances.

It is most likely that a GAIA-type mission will include a carefully optimized medium-band photometry filter set which will allow the determination of accurate effective temperatures and surface gravities, and therefore that the low-resolution spectra described here would not be necessary (except perhaps for peculiar objects, of which such a large-scale spectral survey would be likely to discover large amount, including perhaps even some new classes of objects) to determine this type of information. While at the end the aim should be to extract the primary physical parameters from the target sample, that is, effective temperature, surface gravity and abundance, large scale spectral classification, most likely in some three dimensional system corresponding to these three physical parameters (in the same way as the two dimensional MK system corresponds to temperature and gravity) would still be a useful thing to do, and it could offer some additional astrophysical insights into the target sample.

It is clear that with 50 million objects automatic spectral classification becomes the only possible approach, with reddening being a possible additional complication. So far no fully satisfactory automatic classification algorithms have been reported in the literature which are capable of reliably classifying large number of (possibly noisy) spectra, although many possible approaches are being worked upon by several groups (for a review of current work see Kurtz 1994). It seems likely that an efficient and reliable scheme would however not be impossible to develop, given enough interest and effort.

3. DESIGN IDEAS

Given that the GAIA mission will be operating in a continuous scanning mode (i.e., spinning) it is clear that to maximize simplicity any ‘auxiliary’ instrument should also operate in a similar scanning mode, and at the same scanning rate. Also, the instrument should ideally not have any moving parts. The baseline idea discussed here is to have a slit-less spectrograph, operating in a scanning mode, i.e., with the spectra of all the targets in the field of view continuously scrolling across the detector. To recover the individual pixels in each spectrum there are two basic possibilities: one is to have a detector which time-tags each individual photon, so that by using the attitude information and the time of arrival of each photon the spectrum can be reconstructed (similar to what has been done, for example, for the ROSAT All Sky Survey).

The alternative possibility is to employ a normal 2-D integrating detector (i.e., a CCD), with the columns aligned with the sky scanning direction, and with the pixels being clocked, along the columns, at the exact same rate as the sky scanning rate, so that a pixel in the detector effectively ‘follows’ a sky element. This technique, known as Time Delayed Integration (TDI) has been used from the ground for both imaging and spectral work. For example, Schneider et al. (1994) have carried out a survey to search for faint, high-redshift QSOs at the Mount Palomar 200-inch reflector, by performing low-resolution (using a grism) slit-less spectroscopy of all the objects drifting across the field of view. The telescope was operated, in this context, as a meridian circle, with the hour drive turned off, using the earth rotation to perform the scanning. The Sloan Survey is also using the same principle for the photometric sky scans (Kent et al. 1993).

For a space-based system the implications for the along-scan and transverse satellite attitude control would need to be considered. The along-scan attitude control requirements are unlikely to be more stringent than the acceleration constraints on the interferometers themselves, while the transverse attitude requirements could potentially be as demanding (or more) as the ones of the interferometers. The scan rate is, as shown later, one of the critical parameters influencing the performance of a scanning spectrograph operating with CCD detectors. In particular, a slow scanning rate would increase the S/N achievable at the fainter magnitudes for the high-resolution spectroscopy. Conversely, the astrometric stability would be favoured by a faster scanning rate, although the total data rate and/or the detector performance

may be a limiting factor there.

3.1. Telescope Design and Dimensions

The main parameters defining the telescope are going to be the primary mirror size, the image scale at the focal plane, the total (corrected) field of view, the total size of the instrument and, for a ground-based instrument, the mount.

Primary mirror diameter: if the instrument described here is assumed to be flown as part of the instrumentation package of a mission whose primary goal is to perform interferometry, it is clear that the instrument should be small enough so as not to constrain the main purpose of the mission; also, it should be small so as to constrain costs. Even if it should prove more convenient to acquire the data described here through a dedicated ground-based programme, it is obvious that the smaller the telescope the cheaper the programme would be. We have assumed as a baseline design a 1 m diameter primary mirror, i.e., small enough to be integrated into the GAIA instrumentation package. Such a small telescope could also be a relatively cheap ground instrument. We have also explored a 1.5 m primary mirror design; however, as it will be evident later, the diameter of the primary mirror is really not the factor limiting the performance of the system for the space-based option.

Field of view: starting from the assumption that the survey is going to be performed in scanning mode, and given that the total time spent on a given target in an all-sky scanning survey increases linearly with the size of field of view (being given by $\Omega L/4\pi$, where Ω is the solid angle of the field of view and L is the effective survey duration), the telescope design should aim for as wide a field of view as possible. A two-degree diameter corrected field, while certainly large, seems achievable with current reflecting designs, perhaps with the aid of a focal plane dioptric corrector (the new generation fiber spectrograph on the 4 m Anglo Australian Telescope, for example, has a 2 degree field of view, see Taylor 1994). By corrected, we mean such that at least 80% of the energy remains within one detector pixel size (taken to be 1 arcsec, see below).

Image scale and telescope total size: the requirement for image scale is driven by the desire of maximizing the field of view while matching the pixel size of current detectors. We do not see any specific need for resolving the PSF of the telescope; it would be sufficient to have each star image enclosed in a detector pixel (as for the WFPC camera on-board HST). Assuming a detector pixel size of 20 μm , the baseline image scale for the designs discussed here is 50 arcsec/mm. For a 1 m diameter primary mirror, this translates into an f/4 design, i.e., short but today routinely achieved with fast lightweight primary mirrors (as for example in the Vatican Advanced Technology Telescope, see Blanco et al. 1990). A short-focus telescope has the additional advantage of compactness, limiting the total length of the total optical telescope assembly to a couple of meters, being therefore fully consistent with a satellite contained within the Ariane 5 shroud.

Telescope mount: again for the sake of simplicity and

reliability, it is clear that in the space-based configuration the telescope should have a minimum of moving parts, and in particular should be rigidly integrated within the main satellite structure, scanning the sky as it comes by, without any separate pointing capability. In case of a ground-based instrument, given that it should be used as a transit instrument, a very simple mount would be sufficient. In particular, an alt-az mounting would be sufficient, and in principle even the hour drive could be dispensed with.

3.2. Spectrograph Parameters

The types of measurement described in Section 2. lead to two conflicting requirements: high spectral resolution (for the radial velocity measurements) and wide spectral coverage (for the spectral classification). These two requirements cannot easily be reconciled into a single design, so that it seems necessary to have an instrument with two (either interchangeable or parallel) gratings, one for the echelle mode, the other for the low-resolution mode. While a system in which the grating is changed to allow either low or high resolution spectral data to be collected is surely simpler, parallel acquisition of high and low spectral resolution data is by far the preferred option because it would allow to keep collecting radial velocity measurements for the complete mission duration, thus extending the sensitivity for the detection of wide binary systems. Given the uncertain total duration of a space mission, parallel acquisition affords much lower risks in case of catastrophic failures, and this option should not be considered as the preferred one in future studies. One possibility in this regard would be to feed two parallel spectrographs using a single telescope. The incoming telescope beam could be split by means of a dichroic splitter, extracting a small spectral region which would be sent to the high-resolution spectrograph, while the rest of the light would be fed to the low-resolution spectrograph.

We have nevertheless considered in our simulation, for simplicity, as baseline assumption that about half of the total survey time (5 yr effective time for the current GAIA baseline) would be dedicated to the high-resolution measurements, the other half being dedicated to the low resolution work, thus implying a sequential system switching grating about midway into the planned mission lifetime. A parallel system would therefore allow a longer total integration time (by a factor of about two) for each target object.

3.3. Scanning Rate

On a GAIA-based instrument, the scanning rate of the telescope is fixed by the scanning rate of the main instrument package (the interferometers). The current GAIA baseline assumes 120 arcsec/sec. On a ground-based instrument the scanning rate is fixed by the earth rotation, being 15 arcsec/sec. As will be apparent in the following the scanning rate is a critical parameter, and a relatively low scanning rate (i.e., around the 15 arcsec/sec) offers significant advantages with respect to the relatively high scanning rate of GAIA.

3.4. Detector Performance

As shown below, the detector's performance appears to be the limiting factor in the performance (in terms of limiting magnitude) that can be achieved with a scanning slit-less spectrograph. We will discuss two options, namely a CCD operated TDI mode and a (currently hypothetical) photon counting detector which would time-tag each individual photon.

CCD performance: we have assumed, as baseline performance, current top-of-the-line CCDs. In particular, we are assuming a 2 kpix square device with 80% QE in the red, and a 2 electron read-out noise. We also discuss the benefits to the total spectrograph performance that can be achieved by future CCDs with larger sizes (up to 8 kpix on a side) and (possibly) lower read-out noise.

Photon counting detectors: as will be evident later, the main limiting factor in the total spectrograph performance is actually the detector read-out noise. Therefore a photon counting detector with zero effective read-out noise would be greatly beneficial to such a system. For a GAIA-attached 1 m telescope, for example, going from a 2 electron read-out noise device to a zero-read-out noise device would be able to reach more than 2 mags deeper. The gain is less drastic for a ground-based instrument due to the lower scan speed and correspondingly higher count rates per pixel per second. We will therefore assume, as possible design option, the future availability of high QE photon counting detectors, with a 20 μm effective pixel size, and with the capability to time-tag each individual photon. The time resolution only needs be of the order of the transit time of an individual pixel, i.e., about 50 msec being sufficient. As for the size, again the baseline is a 2 kpix square detector, with the possibility of having detectors as large as 8 kpix being desirable. In the presently discussed configuration a detector with colour discrimination capability does not appear to offer any significant advantage with respect to a colour-blind device such as a normal CCD.

4. SOURCE CONFUSION

One of the potential problems of a slit-less spectrograph is the source confusion, i.e., the overlap between spectra of the different objects. We distinguish here between 'severe' (i.e., non-recoverable) and 'mild' (i.e., recoverable) overlap. Severe overlap occurs whenever two spectra overlap in the dispersion direction, i.e., when they are within 1 arcsec perpendicular to the dispersion direction (assumed here to be 1 arcsec/pix) and within 1 length of the spectrum in the dispersion direction. In this case the two spectra (partly) overlap on the same pixel so that part of the information is lost (even if it maybe be partly recoverable a posteriori by only using the non-overlapped part of the spectra). Mild overlap occurs when the spectra fall at a distance between 1 and 2 pixels perpendicular to the dispersion direction. In this case the wings of each spectrum contaminate the neighbor spectrum (and compromise sky subtraction); this can be corrected for (i.e., by 'smart' sky subtraction) although it is likely to produce degraded S/N for the objects in question.

We have computed the expected fraction of spectra suffering from overlap using an average stellar density as a function of the magnitude (see Allen 1973) and the baseline spectrograph design described here. We have considered all possible overlaps, i.e. even spectra overlapping by a single pixel. The overlap rates given below are therefore in a certain sense worst-case estimates, as in many cases, when the spectra overlap only along a limited number of pixels, much of the information would be recoverable, although at a presumably lower accuracy.

For the high-dispersion mode at $V = 15$ the severe overlap rate is $\approx 3 \times 10^{-3}$, while the mild overlap rate is three times larger, i.e., $\approx 10^{-2}$. Low-resolution spectra are much longer (in our baseline configuration) and therefore more subject to overlap, with severe and mild rates of, respectively, $\approx 1.2 \times 10^{-2}$ and $\approx 4 \times 10^{-2}$. The overlap rates are therefore non negligible, although they are not as large as to jeopardize the feasibility of such a scanning system. The processing of overlapped spectra would be greatly facilitated by the availability of a precise input catalog, which would allow, a priori, to determine which objects are going to be affected, reducing the need for 'intelligent' software. As described in Section 5., the GSC-II would be such a catalog, whose availability seems likely in the time frame of the proposed GAIA mission.

5. TELEMETRY REQUIREMENTS

A continuously scanning instrument generates a continuous stream of data, which, depending on the assumptions made in the design, could put a significant strain on the telemetry requirements of a space-based system. We have computed the raw data flow produced by the scanning spectrograph on the assumption that the CCD is being read with a 20 bit ADC. While high, this number of bits ensures that no saturation is reached for the brighter objects, while still resolving the read-out noise. The raw data rate of the baseline space-based configuration (2 kpix detector, 120 arcsec/sec scan rate) is ≈ 0.5 Mbit/s, increasing to ≈ 2 Mbit/s for a configuration based on a 8 kpix detector. The equivalent ground-based configuration would produce raw data rates of ≈ 0.06 Mbit/s and ≈ 0.24 Mbit/s, respectively, as a result of the lower scan rate.

Given that most of the pixels will be sky pixels, i.e., with a low data value, and only 10% or so of the pixels will contain spectral data, it can be estimated that the effective information content would be approximately 5 bits/pixel, so that through smart data compression schemes the raw data flow could be reduced by a factor of ≈ 4 . More drastic reductions of the data flow would have to be based on on-board processing of the data, i.e., extraction of the spectra and transmission to ground of the extracted, 1-d spectra (possibly with the corresponding extracted sky spectrum). The space-based baseline configuration would produce ≈ 20 spectra/s, corresponding to a nominal data rate of ≈ 80 kbit/s for the echelle case and ≈ 300 kbit/s for the low-resolution case, assuming that the spectra have been re-scaled to a 16 bit range. These nominal rates could be reduced by another factor of two or so by data compression.

The on-board extraction of the spectra, however, would need an input catalog consisting of accurate position and approximate luminosity for the stars being surveyed. Such a catalog will also undoubtedly facilitate the astrometric mission. A useful working assumption appears to be the availability of GSC-II (Lasker, private communication); briefly, the proposed GSC-II programme would provide positions for all 50 million objects (and more) at the sub-arcsec level, out to the year 2020 and beyond.

One possibility to reduce the scan rate for the spectrograph would be to point it at a large angle from the main interferometric package, closer to the spacecraft spin axis. This option, though, would raise several new problems, such as the lack of simultaneity and the uneven sky coverage of an offset instrument, and therefore we will not consider it further.

6. THE ZERO POINT PROBLEM

The determination of the zero-point in a slit-less spectrograph is non trivial, as the precision of final radial velocity determination depends on it. The typical approach on a ground-based objective prism system has been to take two spectra rotating the prism by 180 degs, thus generating two sets of spectra symmetrically shifted from the zero point. This approach is obviously unfeasible in a scanning system. One possible approach would be to reconstruct the zero point from ‘first principles’ using precise astrometry (which will be hopefully available from the GSC-II for all the targets and which would anyway be available with much improved precision a posteriori from the results of the interferometric mission) and the optical parameters of the system. While the requirements on the input catalog astrometry are relatively mild (a 0.5 km/s zero point accuracy translates into 0.06 arcsec astrometric precision on the source catalog), the mechanical stability of the spectrograph should be comparable. For the space-based option, the proposed design, being compact and integrated with the spacecraft, should minimize mechanical stability problems, thermal expansion effects would need to be carefully determined. For the ground-based option, the meridian-circle like configuration should minimize mechanical flexure, although the amount of declination-dependent flexure and thermal expansion would need to be determined.

Another possible approach would be to incorporate a HF gas cell into the light path of the spectrograph, which would provide a set of stable absorption lines superimposed on the stellar spectrum. The HF cell has a good long term stability, and it has been shown to yield a very good zero-point stability (down to ≈ 10 m/s, see for example Campbell et al. 1988). Although HF provides a set of well spaced reference lines with a cell length of less than 1 m, it remains to be investigated whether such a corrosive gas can be reliably used in a space environment.

The usage of a network of traditional radial velocity standard stars for zero-point shift corrections is likely to be a less satisfactory solution, because the velocity stability of each reference object would need to be investigated in detail. High accuracy investigation of standard stars have at times shown the presence

of low amplitude velocity variations (see for example Walker et al. 1989 who find variations of up to 300 m/s rms in the radial velocity of 6 yellow giants, all of which are IAU radial velocity standards) in standard stars, with amplitudes comparable to the expected accuracy of our proposed design for the brighter stars.

7. SUMMARY SPECTROGRAPH DESIGN

The baseline instrument is, in summary, a 1 m diameter Ritchey-Cretien telescope with an f/4 focal length at the Cassegrain focus. The corrected field of view is 2 deg in diameter (if necessary with the aid of a focal plane corrector), and is re-imaged through a conventional slit-less spectrograph using either an echelle grating producing a 7 Å/mm dispersion or a conventional grating producing 100 Å/mm. The passband of the spectrograph should be limited through the use of filters, to about 50 Å for the echelle configuration (basically selecting one echelle order) or to between about 3700 and 7000 Å for the lower resolution. The objects will drift into the field of view at the scan rate, and the spectra will be recorded either using a conventional CCD in TDI mode or by using a photon counting detector.

8. PERFORMANCE

To evaluate the performance of the system we have produced plots of the S/N ratio that can be reached, as a function of the object’s magnitude, both for a single scanning pass and for the total number of passes achieved throughout the lifetime of the system. Each plot shows three curves: the continuous line is the total system performance with a 2 electron read-out noise CCD, the intermediate dashed curve is the total system performance with a zero read-out noise detector, while the uppermost dashed line is the (purely theoretical) performance in a situation with neither read-out noise nor sky background.

8.1. Assumed Throughput and Sky Background

In all the computation we have assumed a total system throughput (telescope plus spectrograph plus detector) of 5% for the echelle configuration, and of 20% for the low-resolution configuration. While relatively high, these throughput levels should be achievable in an optimized system. The assumed sky background is 20 mag per square arcsec, typical of a quarter moon night at a good site. While an orbiting instrument would typically be subject to a lower background, it will be seen that the sky background is not the dominant noise contribution.

8.2. The Performance of the Space-Based Baseline Configuration

The performance of the baseline configuration for the echelle grating is shown in Figure 1, for a 120 arc-sec/sec scanning rate. It can be seen from the left

panel that a single scan (lasting about 15 sec) is enough to produce a usable (i.e., S/N of 5 per pixel) spectrum for a $V \approx 11$ star, with minimal noise contributions from either the sky or the detector read-out noise. Assuming that 2.5 years (i.e., half of the mission's lifetime) are dedicated to the echelle mode, each object would be observed 35 times. Because the read-out noise does not scale down with the total exposure time, the limiting magnitude for the total mission is only $V \approx 12.5$, a gain of only 1.5 mag. However, as apparent from the right panel, a zero read-out noise detector would be able to reach $V \approx 15$, i.e., approximately the same limiting magnitude as the GAIA interferometer. One option to achieve a deeper limiting magnitude (apart from increasing the telescope size, with its obvious impacts on mass and cost) is to have a larger detector, which would increase the duration of each scan, therefore reducing the read-out noise contribution. Notice that a mosaic of CCD's broken along the rows would not have much beneficial effect, as the read-out noise would not decrease. However, a mosaic of long, narrow CCDs butted along the scanning direction would be perfectly adequate. We have therefore considered the case of an 8 kpix square detector, covering the full 2 degree field of view (although any rectangular combination of two-side butted CCDs would be usable). As shown in Figure 2 the limiting magnitude in a single scan goes down to 12.5, while for the total mission reaches $V \approx 14$. The deeper limiting magnitude per scan is due to the longer duration of the scan (about 1 min); note that the larger detector's size across the scanning direction has the effect of increasing the number of scans per object to 140 (from the 35 of the 2 kpix square detector). The read-out noise contribution at the fainter magnitudes is proportionally larger, and a zero read-out noise detector in this configuration could reach $V \approx 16.5$.

The performance of the baseline design for the low resolution spectroscopy is shown in Figure 3. The much lower resolution increases the count rate so that $V \approx 14$ can be easily reached per pass, and $V \geq 15$ can be easily reached in the mission's lifetime. At the lower resolution the read-out noise becomes a negligible contribution, while the much larger spectral bandpass pushes the sky contribution to a significant level, i.e., about 2 mag decrease in performance at a limit S/N of 5. An 8 kpix detector (not shown) would increase the performance even further.

8.3. The Performance of the Ground-Based Baseline Configuration

A similar ground-based instrument would perform differently because of the much lower sidereal scanning rate (15 arcsec/sec) which would make each scan last more than 2 min for the 2 kpix detector, and almost 9 min for the 8 kpix detector. The longer scans significantly improve the performance as they help beat the read-out noise down. As can be seen from Figure 4 the limiting magnitude per scan is down to $V \approx 13.5$. Assuming that a ground-based system would be operating for 2.5 years and would have to observe only half of the sky, it could at most make 3 scans per object, reaching a limiting magnitude of $V \approx 14$. The performance of a similar system with a 8 kpix detector is shown in Figure 5. Such a system would comfortably reach $V \approx 14$ per scan, and

$V \approx 16$ for the 14 scans achievable during the 2.5 years. Given the longer duration of each scan, in the ground-based configuration the benefit of a zero read-out noise detector would be minimal, yielding a gain of half a mag or so.

The performance of a ground-based scanning low-resolution spectrograph is shown in Figure 6. The limiting magnitude per scan is in this case comfortably down to $V \approx 15$, because of the longer scan time, but does not significantly improve in the 3 scans total that would be performed from ground in the survey's lifetime. The end performance of the space and ground-based options is in the case of the low resolution spectroscopy equivalent, as, given that the read-out noise is negligible, exposures can be broken up in different ways without significantly changing the final S/N.

8.4. Performance Improvements

Our baseline calculations are based on a 5% absolute throughput for the high spectral resolution spectrograph and a 20% absolute throughput for the low spectral resolution one. To push the magnitude limit further down, any increase in the collection area in the space-based option would come at very large prices, and it is therefore clear that any improvement in the overall system throughput would be of large benefit. The large difference in assumed throughput between the high and low resolution spectrographs comes mostly from the additional dispersing element which the echelle system needs to separate the various orders. Various possibilities exist to increase the echelle throughput pushing the magnitude limit down; given that only a small spectral region would be used from the echelle spectrum, one possibility would be to dispense with the cross disperser altogether and actually use an order sorting filter selecting the spectral range of interest. Alternatively, if one could obtain a comparable spectral resolution with a conventional, single order spectrograph design, it is likely that the total system throughput could be pushed to values comparable to the low resolution design. While "conventional" holographic gratings suffer from low efficiency, it is not unlikely that improvement in the technology (as for example from the development of ion etching techniques) could bring them into the same efficiency ranges as conventional ruled gratings. If the holographic techniques would progress sufficiently as to produce gratings with high enough groove density (i.e. > 5000 grooves/mm) so that the high resolution spectra could be produced from a single grating design, this would likely mean an improvement in limiting magnitude of about a magnitude or so.

By using holographic gratings, it would also be possible to think about more sophisticated designs, such as Rowland circle spectrographs (as for example has been proposed for the Lyman observatory, see Jakobsen 1988)), which could gain additional throughput by foregoing the camera altogether, although the aberrations of such systems would need to be carefully studied. One additional advantage of a Rowland circle spectrograph would be that, by producing linear, non cross-dispersed spectra, it would be relatively easy to sample two (or more) distinct spectral regions by having two detector systems side by side.

At discussed in Sec. 3.4., the read-out noise of the CCD is a major limiting factor to the performance of the system. It is worth mentioning that there are developments aiming at pushing the read-out noise of CCDs significantly *below* 1 electron through the usage of non-destructive readout amplifiers (see Janesick & Elliott 1992), thus approaching the performance of photon-counting detectors. The availability of such devices could also contribute to push the magnitude limit of the system proposed here further down.

Finally, it has been suggested that our calculations could be overly pessimistic because they do not account for the lack of atmospheric scintillation in space (Grenon, private communication), which could yield an additional performance gain for the space-based configuration compared to the ground based one.

8.5. Summary Performance: Space Or Ground-Based?

Table 1 contains a summary of the key performance parameters for the baseline and enhanced configurations discussed here.

The trade-offs between a ground-based and a ground-based option will need to be evaluated with care; while it is evident that a ground-based system has a considerable advantage in terms of raw limiting magnitude, much of this advantage comes from the lower scanning rate, so that the actual gain will need to be re-assessed in the light of a less preliminary spacecraft design. Also, the possible future availability of a zero read-out noise detector would cancel the magnitude disadvantage of the space-based configuration. The space based configuration has the advantage of a much stabler environment: the low-resolution spectra so collected would for example be immediately available in terms of absolute flux, forming a very large database of absolutely calibrated spectro-photometric information; the level of calibration achievable from a stable platform outside the earth atmosphere would be very difficult to achieve from a ground-based telescope with all the uncertainties related to the variation of the atmospheric transmission (a similar conclusion has been drawn from the photometric data acquired from Hipparcos).

9. CONCLUSIONS

The limits of a space-based 1-m telescope, in the domain considered here, come out, even without careful optimisation, tantalisingly close to values of great astrophysical interest, with a magnitude limit comparable to that motivating the GAIA mission. One aspect that should be carefully considered is the satellite spin rate: for the astrometric rigidity a higher spin rate, detector considerations aside, is more desirable; in contrast, the limiting magnitude of the system considered here increases significantly with decreased spin rate.

The acquisition of these auxiliary data on ground versus their acquisition in space is bound to be a non-trivial question. On the one hand, focussing the goals

of a future space mission exclusively on the astrometric data may be turning our backs on the true potential of such a mission. Considering the two as a single package may make the mission considerably more appealing to a broader scientific group. The experiment could be considered as institute-provided, being decoupled from the astrometric interferometers, and therefore of interest to instrument builders within Europe. The analysis of the resulting data would be an enormous challenge for software reduction, automated analysis and classification systems, and may therefore be of further scientific appeal. While such an option could not be allowed to jeopardize what is already likely to be a challenging project, enlarging the mission's vision should certainly be considered as an important part of a cornerstone mission definition. Proposing the project as a ground-based programme would create different but correspondingly significant problems: how would such an experiment be motivated, coordinated, funded, and exploited? On what time-scale could it be completed, etc?

Given the evident importance of the auxiliary data described here for any comprehensive exploitation of the astrometric data, we consider that further consideration of acquiring such data, in the same 'package' (either on ground or from space) is merited.

ACKNOWLEDGMENTS

We thank M. Grenon, P. Jakobsen, L. Lindgren, M. Lattanzi and C. Turon for the useful comments on early versions of this paper.

References

- Allen, C. 1973, *Astrophysical quantities*, Athlone Press
- Batten, A. H. 1985, in A. G. D. Philip, D. W. Latham (eds.), *Stellar Radial Velocities*, Vol. 88 of *IAU Colloquium*, Davis, Shenectedy, 325
- Blanco, D., Corbally, C., Nagel, R., Woolf, N. 1990, in *Advanced technology optical telescopes IV*, Society of Photo-Optical Instrumentation Engineers, Bellingham, p. 905
- Campbell, B., Walker, G., Yang 1988, *ApJ*, 331, 902
- Carney, B., Laird, J., Latham, D., Kurucz, R. 1987, *AJ*, 94(4), 1066
- Gerbaldi, P., Gómez, A., Grenier, S., Turon, C., Faraggiana, R. 1989, *The ESO Messenger*, 58, 12
- Jakobsen, P. 1988, *Lyman: report on the Phase A Study*, Technical Report SCI(88)3, ESA
- Janesick, J., Elliott, T. 1992, in S. Howell (ed.), *Astronomical CCD observing and reduction techniques*, Vol. 23, *Astronomical CCD observing and reduction techniques of ASP Conference Series*, San Francisco, p. 105
- Kent, S. M., Stoughton, C., Newberg, H., Loveday, J., Petravick, D., Gurbani, V., Berman, E., Sergey, G., Lupton, R. 1993, in D. Crabtree (ed.), *3rd Annual Conference on Astronomical Data Analysis Software and Systems*, ASP, San Francisco

Configuration	R	\approx lim. V single scan	\approx lim. V total
baseline space-based, 2 kpix CCD	30,000	11.0	12.5
baseline space-based, 2 kpix zero read-out noise det.	30,000	11.0	15.0
baseline space-based, 8 kpix CCD	30,000	12.5	14.5
baseline space-based, 2 kpix CCD	1,000	14.0	15.5
baseline ground-based, 2 kpix CCD	30,000	13.0	14.0
baseline ground-based, 8 kpix CCD	30,000	14.0	15.5
baseline ground-based, 2 kpix CCD	1,000	15.0	16.0

Table 1: Summary performance parameters. The faintest achievable magnitude is (for either single or multiple scans) for $S/N=5$.

Kurtz, M. 1994, in J. Bergeron (ed.), Reports on Astronomy, Vol. XXIIA, Kluwer, in press

Lindgren, L., Perryman, M. 1994, The GAIA mission, Technical report

Mayor, M., Duquenooy, A., Grenon, M., Turon, C., Crifo, F., Imbert, M., Maurice, E., Prevot, L., Andersen, J., Nordstrom, B., Lindgren, H. 1989, The ESO Messenger, 58, 12

Perryman, M. 1994, in IAU Symp. 166, in press

Pinsonneault, M., Kawaler, S., Demarque, P. 1990, ApJS, 74, 501

Schneider, D. P., Schmidt, M., Gunn, J. E. 1994, AJ, 107(1245)

Soderblom, D., Jones, B., Balachandran, S., Stauffer, J., Duncan, D., Fedele, S., Hudon, J. 1993, AJ, 106, 1059

Taylor, K. 1994, AAO Newsletter, 69

Walker, G., Yang, S., Campbell, B., Irwin, A. 1989, ApJ, 343, L21

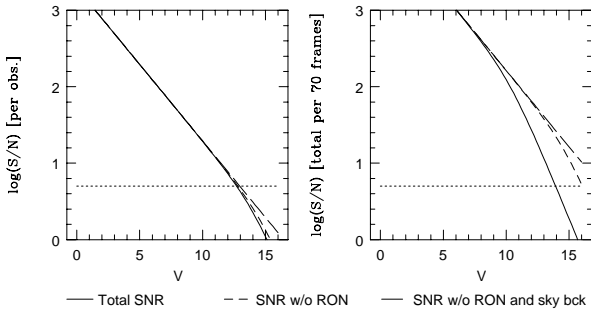


Figure 1: The performance of the baseline configuration for the space-based echelle measurements

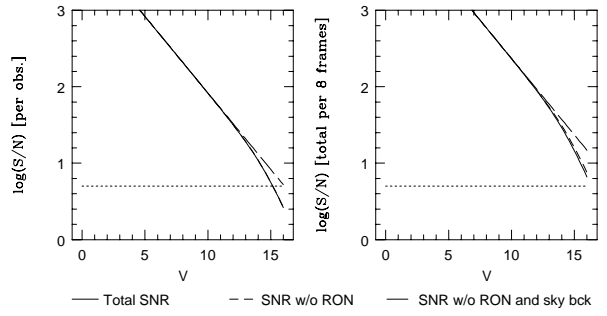


Figure 4: The performance of the baseline configuration for the ground-based echelle measurements

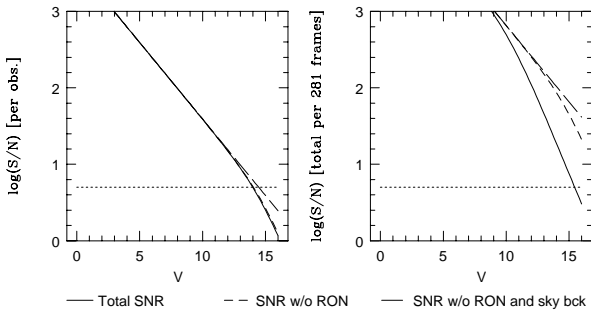


Figure 2: The performance of the baseline configuration for the space-based echelle measurements with a 8 kpix detector

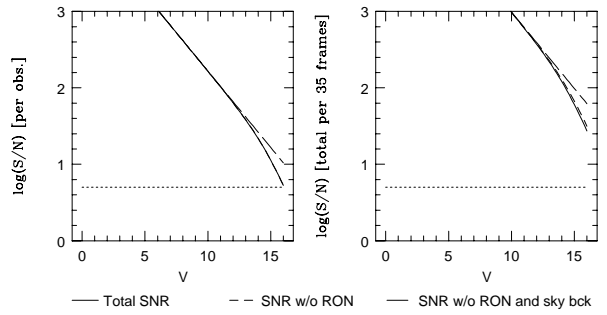


Figure 5: The performance of the baseline configuration for the ground-based echelle measurements with a 8 kpix detector

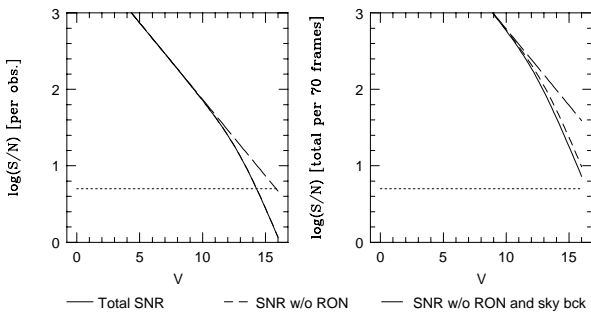


Figure 3: The performance of the baseline configuration for the space-based low-res measurements

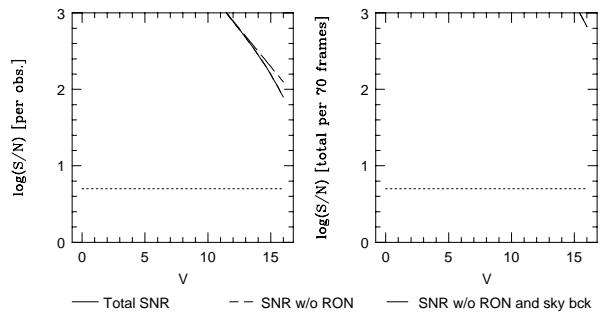


Figure 6: The performance of the baseline configuration for the ground-based low-res measurements

RON = 2
 2000 X 2000 pix det.
 1 m diam. scope
 System eff. 0.2
 Track. rate 120 arcsec/sec
 Spectral disp. 7 A/mm
 Eff. wavelength 5500 A
 Spectral coverage 40 A
 Sky bck 21 mag/as**2
 Image scale 50 arcsec/mm
 1 arcsec pixels
 Detector pix size 20 microm
 ADU resolution 20 bits
 Minimum useful SNR 5

Integ. per pass 16.6667 sec
 Tot. integ. per obj 1173.71 sec
 Passes per obj 70
 Spectral res 0.14 A/pix
 Veloc. res. 0.763636 km/sec
 FOV 33.3333 X 33.3333 arcmin
 Effective survey duration 5 yrs
 Total data rate 0.48 Mbit/sec
 Spectrum length 285.714 pix
 CCD clocked at 120 pix/sec

RON = 2
 2000 X 2000 pix det.
 1.5 m diam. scope
 System eff. 0.2
 Track. rate 15 arcsec/sec
 Spectral disp. 7 A/mm
 Eff. wavelength 5500 A
 Spectral coverage 40 A
 Sky bck 21 mag/as**2
 Image scale 50 arcsec/mm
 1 arcsec pixels
 Detector pix size 20 microm
 ADU resolution 20 bits
 Minimum useful SNR 5

Integ. per pass 133.333 sec
 Tot. integ. per obj 1173.71 sec
 Passes per obj 8
 Spectral res 0.14 A/pix
 Veloc. res. 0.763636 km/sec
 FOV 33.3333 X 33.3333 arcmin
 Effective survey duration 5 yrs
 Total data rate 0.06 Mbit/sec
 Spectrum length 285.714 pix
 CCD clocked at 15 pix/sec

Figure 7: The parameter set used for computing the performance of the baseline configuration for the space-based echelle measurements

Figure 10: The parameter set used for computing the performance of the baseline configuration for the ground-based echelle measurements

RON = 2
 8000 X 8000 pix det.
 1 m diam. scope
 System eff. 0.2
 Track. rate 120 arcsec/sec
 Spectral disp. 7 A/mm
 Eff. wavelength 5500 A
 Spectral coverage 40 A
 Sky bck 21 mag/as**2
 Image scale 50 arcsec/mm
 1 arcsec pixels
 Detector pix size 20 microm
 ADU resolution 20 bits
 Minimum useful SNR 5

Integ. per pass 66.6667 sec
 Tot. integ. per obj 18779.4 sec
 Passes per obj 281
 Spectral res 0.14 A/pix
 Veloc. res. 0.763636 km/sec
 FOV 133.333 X 133.333 arcmin
 Effective survey duration 5 yrs
 Total data rate 1.92 Mbit/sec
 Spectrum length 285.714 pix
 CCD clocked at 120 pix/sec

RON = 2
 8000 X 8000 pix det.
 1.5 m diam. scope
 System eff. 0.2
 Track. rate 15 arcsec/sec
 Spectral disp. 7 A/mm
 Eff. wavelength 5500 A
 Spectral coverage 40 A
 Sky bck 21 mag/as**2
 Image scale 50 arcsec/mm
 1 arcsec pixels
 Detector pix size 20 microm
 ADU resolution 20 bits
 Minimum useful SNR 5

Integ. per pass 533.333 sec
 Tot. integ. per obj 18779.4 sec
 Passes per obj 35
 Spectral res 0.14 A/pix
 Veloc. res. 0.763636 km/sec
 FOV 133.333 X 133.333 arcmin
 Effective survey duration 5 yrs
 Total data rate 0.24 Mbit/sec
 Spectrum length 285.714 pix
 CCD clocked at 15 pix/sec

Figure 8: The parameter set used for computing the performance of the baseline configuration for the space-based echelle measurements with a 8 kpix detector

Figure 11: The parameter set used for computing the performance of the baseline configuration for the ground-based echelle measurements with a 8 kpix detector

RON = 2
 2000 X 2000 pix det.
 1 m diam. scope
 System eff. 0.2
 Track. rate 120 arcsec/sec
 Spectral disp. 100 A/mm
 Eff. wavelength 5500 A
 Spectral coverage 3000 A
 Sky bck 21 mag/as**2
 Image scale 50 arcsec/mm
 1 arcsec pixels
 Detector pix size 20 microm
 ADU resolution 20 bits
 Minimum useful SNR 5

Integ. per pass 16.6667 sec
 Tot. integ. per obj 1173.71 sec
 Passes per obj 70
 Spectral res 2 A/pix
 Veloc. res. 10.9091 km/sec
 FOV 33.3333 X 33.3333 arcmin
 Effective survey duration 5 yrs
 Total data rate 0.48 Mbit/sec
 Spectrum length 1500 pix
 CCD clocked at 120 pix/sec

RON = 2
 8000 X 8000 pix det.
 1.5 m diam. scope
 System eff. 0.2
 Track. rate 15 arcsec/sec
 Spectral disp. 1000 A/mm
 Eff. wavelength 5500 A
 Spectral coverage 3000 A
 Sky bck 21 mag/as**2
 Image scale 50 arcsec/mm
 1 arcsec pixels
 Detector pix size 20 microm
 ADU resolution 20 bits
 Minimum useful SNR 5

Integ. per pass 533.333 sec
 Tot. integ. per obj 37558.7 sec
 Passes per obj 70
 Spectral res 20 A/pix
 Veloc. res. 109.091 km/sec
 FOV 133.333 X 133.333 arcmin
 Effective survey duration 5 yrs
 Total data rate 0.24 Mbit/sec
 Spectrum length 150 pix
 CCD clocked at 15 pix/sec

Figure 9: The performance of the baseline configuration for the space-based low-res measurements

Figure 12: The parameter set used for computing the performance of the baseline configuration for the ground-based low-res measurements